



ELSEVIER

Journal of Alloys and Compounds 323–324 (2001) 618–622

Journal of
ALLOYS
AND COMPOUNDS

www.elsevier.com/locate/jallcom

Structural and electronic characterization of $\text{Nd}_{1.33}\text{Na}_{0.66}\text{Mn}_{0.66}\text{Ti}_{1.34}\text{O}_6$

P. Martín, M.L. López*, A.I. Ruiz, M.L. Veiga, C. Pico

Departamento de Química Inorgánica I, Facultad de Ciencias Químicas, Universidad Complutense, 28040, Madrid, Spain

Abstract

$\text{Nd}_{1.33}\text{Na}_{0.66}\text{Mn}_{0.66}\text{Ti}_{1.34}\text{O}_6$ was synthesised in air and He atmospheres and was characterised by X-ray diffraction by the Rietveld profile analysis. This phase adopts a perovskite-type structure in which Nd and Na are randomly distributed on the A-sites and the Mn and Ti are on the B ones (space group *Pbnm*). The electrical properties show a semiconductor behaviour with low activation energy. Magnetic susceptibility variation with temperature shows antiferromagnetic interactions at 6 K. © 2001 Elsevier Science B.V. All rights reserved.

Keywords: Semiconductors; Chemical synthesis; X-ray diffraction; Magnetic measurements

1. Introduction

Mixed oxides ABO_3 having a perovskite-type structure show octahedral coordination for B atoms and cuboctahedral coordination for A ones, and the parent structure is described in the space group *Pm3m*. A large number of mixed oxides with structures related to the perovskite-type have so far been reported, in which there are deviation from the ideal stoichiometry and very frequently belonging to non-cubic space groups [1]. In this sense, cation vacancies at A sites can exist over a wide range of composition and an ordering of A-site vacancies has been found in some compounds such as $\text{Ln}_{1.33-x}\text{Na}_{3x}\text{Ti}_2\text{O}_6$ [2] and $\text{M}_{1-3x}\text{La}_{1+x}(\text{MgW})\text{O}_6$ [3].

It is well-known that the flexibility of the perovskite and related structures show quite different electrical behaviours as a function of the chemical nature and oxidation states of the elements involved [4].

The aim of this paper is to report the structural characterisation and electrical and magnetic behaviour of the title compound derived from $\text{Ln}_{1.33}\text{Ti}_2\text{O}_6$ where the Ti^{4+} ion is replaced by Mn^{3+} . Na^+ is introduced to the structure to reach the perovskite stoichiometry $(\text{Ln}, \text{Na})_2(\text{B}, \text{B}')_2\text{O}_6$.

2. Experimental

Polycrystalline samples $\text{Nd}_{1.33}\text{Na}_{0.66}\text{Mn}_{0.66}\text{Ti}_{1.34}\text{O}_6$ were prepared by the 'liquid mix' technique [5] from

powdered mixtures of $\text{C}_{15}\text{H}_{21}\text{O}_6\text{Mn}$, $\text{Nd}(\text{NO}_3)_3 \cdot 6\text{H}_2\text{O}$, NaNO_3 and TiO_2 , in stoichiometric ratio, thermally treated at 1173 K for 12 h in air, as described elsewhere [6]. The sample obtained in helium was prepared by the ceramic method at 1073 K for 12 h. The samples were dissolved in $\text{H}_2\text{SO}_4\text{-H}_2\text{O}$ (50:50). The $\text{Mn}^{3+}:\text{Mn}^{4+}$ ratio was obtained by redox titration using an excess of FeSO_4 solution and back titration with potassium permanganate.

Powder diffraction patterns were registered at a rate of $0.2^\circ (2\theta) \text{ min}^{-1}$ by means of a Siemens Kristalloflex diffractometer powered with a D-500 generator using Ni-filtered $\text{CuK}\alpha$ radiation and a 2θ step size of 0.05° with a counting time of 12.5 s for each step. The goniometer was connected to a PC controlled by the commercial program PC-APD (analytical powder diffraction software, 4.0 e). A Rietveld profile analysis method [7] was employed for refining the X-ray diffraction (XRD) results in these materials.

Electrical measurements were carried out with a Solartron 1260 Impedance/Gain phase analyser with a frequency range of 0.1 Hz–10 MHz. Samples were pressed into pellets and then sintered in air at 1073 K for 24 h and in He at 1173 K for 24 h. Blocking electrodes were deposited on both sides of the pellets by platinum paint. Resistance values were derived from an interpretation of the complex impedance plane diagram of the data and measurements in d.c. were carried out using a two-probe technique.

Magnetic susceptibility data were measured with a Squid (Quantum Design, MPMS-XL model) with a sensitivity of 10^{-10} emu in the temperature range 2–300 K (applied field of 1000 Oe).

*Corresponding author.

E-mail address: marisal@eucmax.sim.ucm.es (M.L. López).

3. Results and discussion

A pure phase of composition $\text{Nd}_{1.33}\text{Na}_{0.66}\text{Mn}_{0.66}\text{Ti}_{1.34}\text{O}_6$ was obtained under the experimental conditions described above and chemical analysis confirmed that all the manganese was presented as Mn(III). The sample shows the XRD pattern characteristic of the perovskite structure, in which some reflections are split indicating a distortion from the ideal cubic symmetry. All the reflections could be satisfactorily indexed on the basis of an orthorhombic unit cell, space group *Pbnm*, with the parameters $a_o \approx b_o \approx \sqrt{2} a_p$ and $c_o \approx 2a_p$ (where a_o is the unit cell parameter of the ideal perovskite).

The refined atomic coordinates, unit cell parameters and occupancy *R*-factors obtained are listed in Table 1 and these *R*-factors seem to indicate a reliable structural model. The agreement between the observed and calculated XRD profiles for the air and He samples is shown in Fig. 1. An examination of the refined atomic coordinates, listed in Table 1, shows that Mn and Ti are placed on the ideal sites and the remaining metal atoms are only slightly displaced from their respective ideal positions. Cations in the A-perovskite sites (Na/Nd) and in the B ones (Mn/Ti) will be noted in the following discussion as A and B, respectively. In order to study the distortion around the Mn and

Ti atoms, which are in BO_6 octahedral coordination, the interatomic distances, O–B–O angles and standard deviations were calculated and are listed in Table 2. There are three different B–O sets of bond lengths and the average B–O distance is in good agreement with the sum of the Shannon ionic radii [8]. There are four different O–B–O angles showing a small deviation from the ideal 90° angle for a cubic perovskite. As can be seen from the interatomic distances and angles, the BO_6 octahedra are quite distorted as a consequence of the different nature and charge of the metal cations that are occupying these polyhedra.

On the other hand, neodymium and sodium cations are located in the A sites and inside eight-coordinated polyhedra (Table 2), being quite distorted with respect to the parent cubic structure where the A coordination is twelve. These polyhedra are defined as distorted bicapped prisms which can be related to the cuboctahedral ones by the loss from the latter of four oxygen anions located on four opposite edges in the unit cell. Such a displacement of oxygen anions produces a tilting of BO_6 octahedra in the [001] and [110] directions of the parent structure. The octahedral tilting are close 25° and 20° , respectively.

In summary, from the above structural results, we can conclude that this phase possesses a perovskite-type structure with orthorhombic symmetry in which both Ti and Mn

Table 1

Refined atomic positions, lattice parameters and *R* factors for $\text{Na}_{0.66}\text{Nd}_{1.33}\text{Mn}_{0.66}\text{Ti}_{1.34}\text{O}_6$, obtained by X-ray diffraction

		$\text{Na}_{0.66}\text{Nd}_{1.33}\text{Mn}_{0.66}\text{Ti}_{1.34}\text{O}_6$ (air)	$\text{Na}_{0.66}\text{Nd}_{1.33}\text{Mn}_{0.66}\text{Ti}_{1.34}\text{O}_6$ (He)
Space group		<i>Pbnm</i>	<i>Pbnm</i>
Na/Nd	x (Å)	–0.002(3)	0.005(3)
	y (Å)	–0.021(3)	–0.024(2)
	z (Å)	0.250	0.250
	B (Å ²)	0.356(2)	0.577(5)
Mn/Ti	x (Å)	0.500	0.500
	y (Å)	0.000	0.000
	z (Å)	0.000	0.000
	B (Å ²)	0.099(1)	0.692(6)
O1	x (Å)	–0.080(4)	–0.074(2)
	y (Å)	0.516(5)	0.525(3)
	z (Å)	0.250	0.250
	B (Å ²)	0.487(3)	1.179(3)
O2	x (Å)	0.740(5)	0.735(5)
	y (Å)	0.275(6)	0.281(3)
	Z (Å)	–0.025(4)	–0.038(5)
	B (Å ²)	0.487(4)	1.179(3)
a (Å)		5.438(8)	5.456(8)
b (Å)		5.457(7)	5.484(9)
c (Å)		7.680(9)	7.702(5)
V (Å ³)		227.884	230.452
R_B (%)		6.71	5.73
R_P (%)		11.1	9.22
R_{WP} (%)		16.1	13.2
χ^2		10.7	10.6

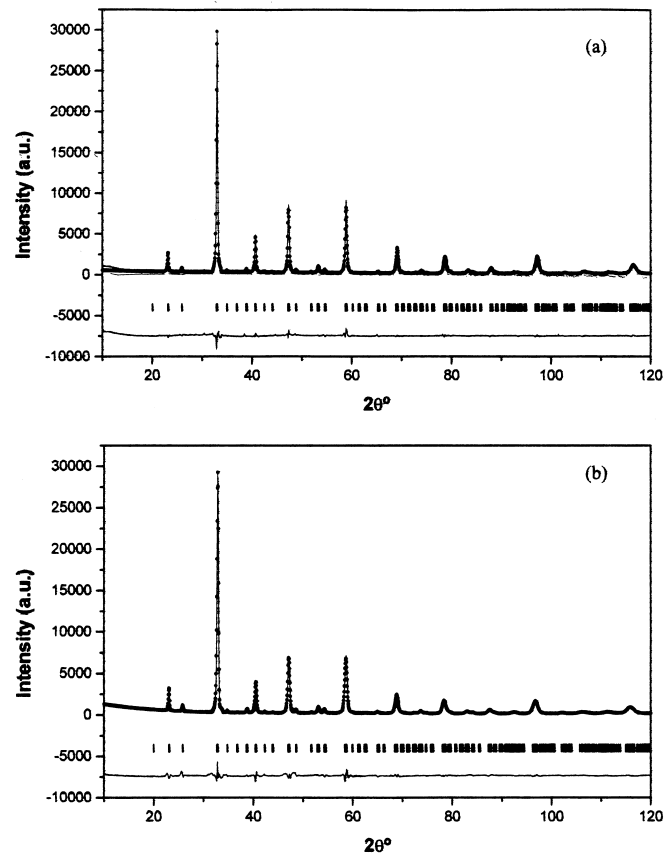


Fig. 1. Calculated (full line) and observed (dots) XRD patterns and difference spectrum for $\text{Na}_{0.66}\text{Nd}_{1.33}\text{Mn}_{0.66}\text{Ti}_{1.34}\text{O}_6$ synthesized in (a) air and (b) He.

Table 2

Interatomic distances (Å) and angles (°) for BO_6 and AO_{12} polyhedra in $\text{Na}_{0.66}\text{Nd}_{1.33}\text{Mn}_{0.66}\text{Ti}_{1.34}\text{O}_6$

	$\text{Na}_{0.66}\text{Nd}_{1.33}\text{Mn}_{0.66}\text{Ti}_{1.34}\text{O}_6$ (air)	$\text{Na}_{0.66}\text{Nd}_{1.33}\text{Mn}_{0.66}\text{Ti}_{1.34}\text{O}_6$ (He)
d (B–O1)	1.971(1) ($\times 2$)	1.972(3) ($\times 2$)
d (B–O2)	1.884(2) ($\times 2$) 1.996(0) ($\times 2$)	1.901(2) ($\times 2$) 2.027(3) ($\times 2$)
Mean	1.950	1.964
Shannon	2.018	2.018
O1–B–O2	85.2(2) ($\times 2$) 87.8(8) ($\times 2$) 92.2(2) ($\times 2$) 94.8(8) ($\times 2$)	87.6(3) ($\times 2$) 87.7(4) ($\times 2$) 92.2(4) ($\times 2$) 92.7(7) ($\times 2$)
O2–B–O2	89.4(0) ($\times 2$) 90.6(9) ($\times 2$)	88.7(8) ($\times 2$) 91.3(1) ($\times 2$)
B–O1–B	153.9(8)	155.2(9)
B–O2–B	166.1(0)	159.9(5)
Mean	159.9	157.6
d (A–O1)	2.301(9) 2.566(9)	2.508(0) 2.369(6)
d (A–O2)	2.544(0) ($\times 2$) 2.620(9) ($\times 2$) 2.726(1) ($\times 2$) 2.581 2.527	2.455(1) ($\times 2$) 2.583(2) ($\times 2$) 2.786(5) ($\times 2$) 2.566 2.527

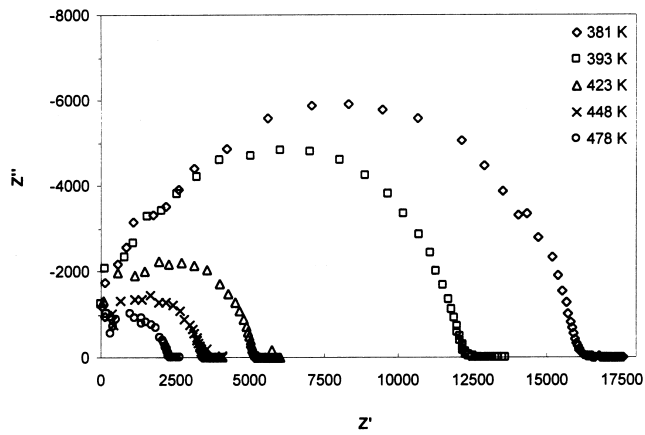


Fig. 2. Complex impedance plots at difference temperatures for $\text{Na}_{0.66}\text{Nd}_{1.33}\text{Mn}_{0.66}\text{Ti}_{1.34}\text{O}_6$ (air).

cations are placed at random in the octahedral B sites whereas La and Na occupies the A sites in eight-coordination.

3.1. Electrical properties

Measurements of a.c. impedance spectra have been carried out by alternating current techniques from the complex impedance (Z) plots [9]. Fig. 2 shows the Z'' (imaginary part) vs. Z' (real part) for the sample obtained in helium which is similar to the corresponding graph for the air sample; the semicircle is somewhat depressed at this latter temperature. For all temperatures measured, a semicircle and a spike at low frequencies which is over the

Z' -axis, were observed. This phenomenon indicates that a non electrode–electrolyte response exists.

Conductivity values for both samples were determined from the complex impedance plots over a wide range of temperatures and they can be fitted to an Arrhenius equation of the form: $\sigma = \sigma_0 \cdot \exp(-E_a/kT)$. Fig. 3 shows the linear plots of $\log \sigma T$ vs. $1000/T$ for both samples. Measurements in d.c. were also carried out on the same sample and electrodes which were used for a.c. measurements. The results were very close to the a.c. ones and the Arrhenius fit of both measurements are gathered in Fig. 3. The activation energy is 0.31 eV for the air sample and 0.30 eV for the He one, which is indicative of good conduction. The difference was due to the different cell constants of the two measured samples.

3.2. Magnetic properties

Fig. 4 shows the temperature dependence of the magnetic susceptibility of $\text{Na}_{0.66}\text{Nd}_{1.33}\text{Mn}_{0.66}\text{Ti}_{1.34}\text{O}_6$ obtained in an He atmosphere. The susceptibility remains almost constant between 300 and 75 K, while a marked increase is detected at lower temperatures showing a maximum at about 5 K. This maximum suggests the presence of antiferromagnetic interactions that can be attributed to the Mn^{3+} contribution.

The temperature dependence of the reciprocal susceptibility for $\text{Na}_{0.66}\text{Nd}_{1.33}\text{Mn}_{0.66}\text{Ti}_{1.34}\text{O}_6$ is shown in Fig. 4. The susceptibility follows a Curie–Weiss behaviour over a very wide range of temperatures, i.e. 300–75 K. The obtained magnetic moment of $6.15 \mu_B$ is very close to $5.82 \mu_B$, which is the expected value for $\text{Ln}^{3+}/\text{Mn}^{3+}$ calculated

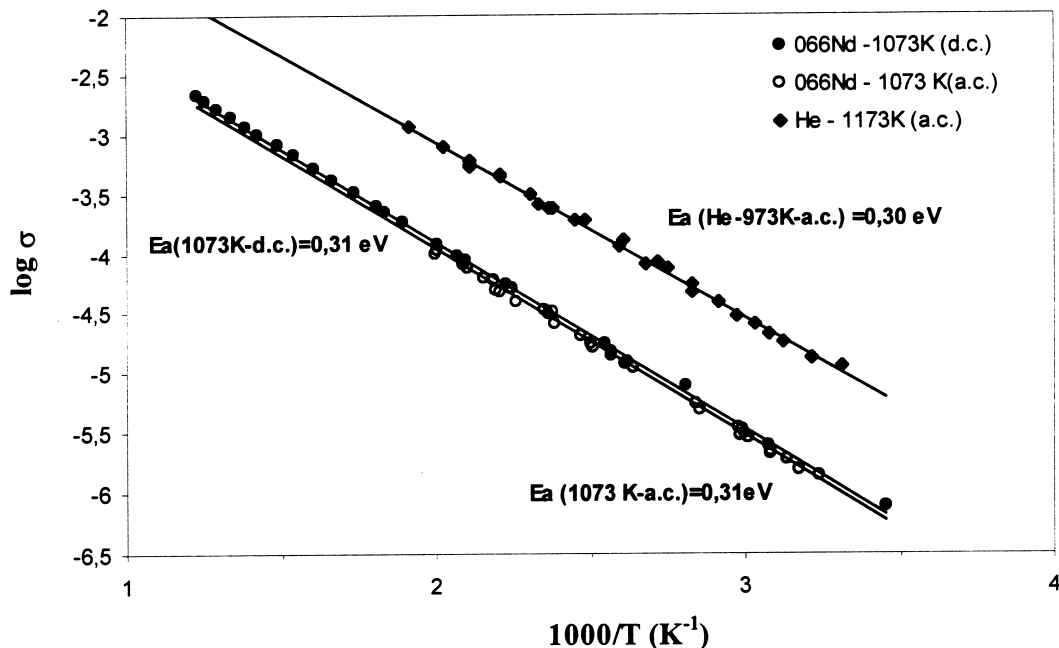


Fig. 3. Arrhenius plots for the sample $\text{Na}_{0.66}\text{Nd}_{1.33}\text{Mn}_{0.66}\text{Ti}_{1.34}\text{O}_6$ (air and He atmospheres).

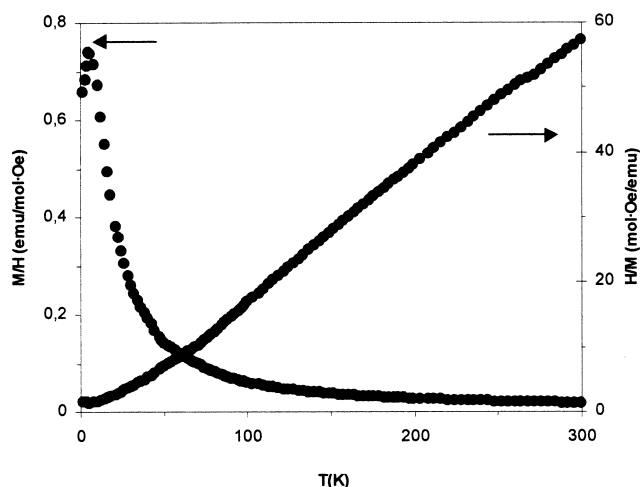


Fig. 4. Susceptibility and reciprocal susceptibility vs. temperature curve for $\text{Na}_{0.66}\text{Nd}_{1.33}\text{Mn}_{0.66}\text{Ti}_{1.34}\text{O}_6$ (He).

from the expression $\mu_t = [x \cdot (\mu_{\text{Mn}^{3+}}^2) + 1.33 \cdot (\mu_{\text{Ln}^{3+}}^2)]^{1/2}$ ($\mu_{\text{Mn}^{3+}}$ and $\mu_{\text{Ln}^{3+}}$ being the magnetic moments for the respective free ions).

4. Conclusion

In order to investigate the influence of the synthesis conditions on the properties, the compound $\text{Na}_{0.66}\text{Nd}_{1.33}\text{Mn}_{0.66}\text{Ti}_{1.34}\text{O}_6$ was prepared in air and in He atmospheres. From the X-ray powder diffraction data, the symmetry of both samples are orthorhombic with the space group $Pbnm$ and have no noticeable structural differences.

The title compound behaves as a good conductor, with relatively low activation energy. Due to the absence of vacancies in the A sites, the conductivity is purely

electronic. From a.c. measurements we can conclude that the atmosphere of the synthesis does not influence the electrical properties of the compound $\text{Na}_{0.66}\text{Nd}_{1.33}\text{Mn}_{0.66}\text{Ti}_{1.34}\text{O}_6$, as shown by the similar activation energies values of the samples prepared in air and He.

From magnetic measurements it can be concluded that antiferromagnetic interactions at 6 K, due to coupling between the Mn^{3+} ions that are located on the B sites and the Nd^{3+} in the A sublattice. Besides, the positive value of the Weiss constant, could indicate that this sample present an antiferromagnetic ordering with a very weak ferromagnetic canting.

Acknowledgements

Financial support from CICYT (Grant Mat2000-1585-C03-02) is gratefully acknowledged.

References

- [1] M.L. López, A. Jerez, C. Pico, R. Saez-Puche, M.L. Veiga, J. Solid State Chem. 105 (1993) 19.
- [2] A.I. Ruiz, M.L. López, M.L. Veiga, C. Pico, Solid State Ionics 112 (1998) 291.
- [3] M.A. Arillo, J. Gómez, M.L. López, C. Pico, M.L. Veiga, Solid State Ionics 95 (1997) 241.
- [4] A.I. Ruiz, M.L. López, M.L. Veiga, C. Pico, Eur. J. Inorg. Chem. (2000) 656–664.
- [5] M. Pechini, US Pat. 3,231, 1966, 328.
- [6] I. Álvarez, M.L. Veiga, C. Pico, J. Alloys Comp. 255 (1997) 74.
- [7] J. Rodríguez-Carvajal, Physica (Amsterdam) 192B (1993) 55.
- [8] R.D. Shannon, Acta Cryst. A32 (1996) 75.
- [9] Zview, Graphics and Analysis Dotware, Scribner Associates, 1994.